Decomposition of powerful axisymmetrically polarized laser pulses in underdense plasma

Nobuhiko Nakanii, Tomonao Hosokai, Naveen C. Pathak, Shinichi Masuda, Alexei G. Zhidkov, Hiroki Nakahara, Kenta Iwasa, Yoshio Mizuta, Naoki Takeguchi, Takamitsu P. Otsuka, Keiichi Sueda, Jumpei Ogino, Hirotaka Nakamura, Michiaki Mori, Masaki Kando, and Ryosuke Kodama

Insight of decomposition of powerful axisymmetrically-polarized laser pulses in under-dense plasma

Nobuhiko Nakanii,[1,2,3,*] Tomonao Hosokai,[4,1,2] Naveen C. Pathak,[1] Shinichi
Masuda,[1,2] Alexei G. Zhidkov,[1,2] Hiroki Nakahara,[4] Kenta Iwasa,[4] Yoshio Mizuta,[4]
Naoki Takeguchi,[4] Takamitsu P. Otsuka,[1] Keiichi Sueda,[1] Jumpei Ogino,[1]
Hirotaka Nakamura,[4] Michiaki Mori,[3] Masaki Kando,[3] and Ryosuke Kodama[4,1,5]

[1]*Photon Pioneers Center, Osaka University*

[2]*CREST, Japan Science and Technology Agency*

[3]*Kansai Photon Science Institute, National Institutes*
for Quantum and Radiological Science and Technology

[4]*Graduate School of Engineering, Osaka University*

[5]*Institute of Laser Engineering, Osaka University*

(Dated: October 17, 2016)

Abstract

Interaction of relativistically intense axisymmetrically-polarized (radially or azimuthally-polarized) laser pulses (RIAPL) with under-dense plasma is shown experimentally and theoretically to be essentially different from the interaction of conventional Gaussian pulses. The difference is clearly observed in distinct spectra of the side scattered laser light for the RIAPL and Gaussian pulses, as well as, in appearance of a spatially localized strong side emission of second harmonic of the laser pulse in the case of RIAPL. According to our analysis based on 3D particle-in-cell simulations, this is a result of instability in the propagation of RIAPL in uniform under-dense plasma.

* nakanii.nobuhiko@qst.go.jp; Current affiliation: Kansai Photon Science Institute, National Institutes for Quantum and Radiological Science and Technology

Quality of laser filed distribution is a key part of any laser technique. For example, Gaussian-shape laser pulses are widely used for laser wakefield acceleration (LWFA)[1-9] because of their high quality. Propagation of Gaussian laser pulses in under-dense plasma was a matter of study for decades. Self-focusing, filamentation, and hosing are well investigated for high power short laser pulses with the Gaussian profile [10-12]. However, some laser modes may be useful for controllable electron self-injection, further electron acceleration and/or probing of quality of plasma optics[13-15]. Here, axisymmetrically-polarized, radially (E_r, B_ϕ) or azimuthally-polarized (E_ϕ, B_r), laser pulses are of particular interest being two TEM01 or TEM10 modes, the nearest to Gaussian (TEM00) mode. Such modes when tightly focused have been proposed theoretically for the electron vacuum acceleration [16-18] and for efficient electron/positron wakefield acceleration [19]. However, the propagation of relativistically intense axisymmetrically-polarized laser pulse (RIAPL) in underdense plasma has particularly interest in view of existence of different laser mode in plasma. To our knowledge, effects of propagation such pulses in under-dense plasma have yet to be examined both theoretically and experimentally.

Intensity of axisymmetrically-polarized laser pulses has donut-shape in a pulse focal spot. The transverse ponderomotive force of the RIAPL, acting towards the laser axis, can collect large number of electrons into the central limited area of the spot [19, 20]. The increase of charge density of electron beam can be expected due to injecting these massive electrons to wake-field excited by another laser pulse in staging acceleration, on the other hand, the electron compression at the laser axis can cause instability, the decomposition of the RIAPL, as predicted in Ref. [20].

In this paper, we demonstrate experimental proof of the RIAPL decomposition, which being manifested in strong side emission of second harmonics generation from the compressed high-density electrons. And also shown this via spectral analysis of laser electric field using three dimensional relativistic particle-in-cell simulation.

Experimental setup is shown in Fig. 1(a). This experiment has been performed with a 40-TW Ti:Sapphire laser system (Amplitude Technologies) at Photon Pioneers Center, Osaka University based on a chirped pulse amplification (CPA) technique. The pulse energy on target was 660 mJ and the pulse duration was 50 fs. The central wavelength of the laser pulse is 800 nm. The contrast ratio between the main pulse and the nanosecond pre-pulse caused by the amplified spontaneous emission (ASE) is $\sim 10^{10}$. The contrast at 1 ps and 10 ps before

the peak of main pulse is $\sim 10^5$ and 10^9, respectively. Those are measured by third-order cross correlator (SEQOIA, Amplitude Technology). The maximum laser intensity of the RIAPL on the target is estimated to be 3×10^{19} W/cm^2. A linearly-polarized(horizontally-polarized) laser pulse with diameter of ~ 50 mm is converted to axisymmetrically-polarized laser pulse by passing through an 8-divided wave-plate [22, 23]. As shown in Fig.1 (b), the 8-divided wave-plate is consisted from 8 pieces of $1/2\ \lambda$ wave-plate with different optical axis. Rotating the wave-plate enables to switch the pulse polarization between radial, azimuth and the spiral polarizations. The RIAPL is focused at a distance of 100 μm inside from the front edge of the slit nozzle by a gold-coated off-axis parabolic mirror (OAP) with f/3.6 (f = 177.8 mm). The focal spot patterns in vacuum with/without using the 8-divided waveplate on target measured by focal spot monitor are shown in Fig.1(c) and (d), respectively. The focal spot of the RIAPL has clearly donut shape, otherwise that of the relativistically intense linearly-polarized laser pulse(RILPL) has gaussian shape.

The pulsed gas jet of helium is produced by a shock-wave-free slit nozzle and solenoid valve (Smartshell Co.). The shape of nozzle exit is rectangular of 1.2 mm length and 4.0 mm width. The atomic density of the gas is estimated to be about 3.4×10^{19} cm^{-3}. The gas could be fully ionized by the laser pulse. A magnetic device which consists of two ring-shaped neodymium magnets applies external magnetic field (B ~ 0.25 T) in laser propagation direction [24-26]. The spatial distribution of ejected electron beams as an important characteristic of laser-plasma interaction was measured by a phosphor screen (Mitsubishi Chemical Co. LTD, DRZ-High) with diameter of 9 cm. The screen is located at 43 cm away from the gas jet target. The DRZ-High screen is sensitive to high-energy particles and radiations, so that the front side of the screen is laminated with a 12-μm-thick aluminum foil to avoid exposure to the laser pulses, scattering lights and low-energy electrons. An electron spectrometer using a dipole magnet measures the energy spectrum of the beams. The energy-resolved electrons turned by the dipole magnet (B ~ 0.25 T) irradiates to another phosphor screen. A 1-cm-thick aluminum collimator with 5-mm-diameter hole is placed in front of the electron spectrometer. The scintillating images on these phosphor screens made by the deposited electrons are recorded by charged coupled device (CCD) cameras (Bitran Co., BU-51LN) with a commercial photographic lens from the backside of the screen. To reduce the background noise due to scattering light of laser pulses, band-pass filters (BG-39, $\lambda = 360$ - 580 nm) are set at the front of the cameras.
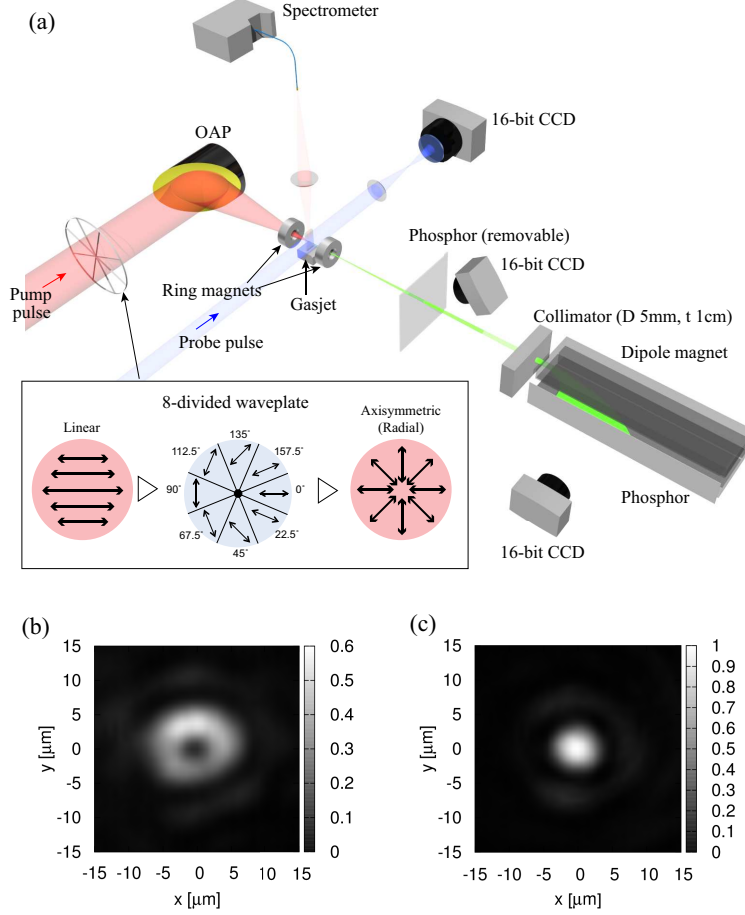
FIG. 1. (a) Experimental schematic (b) Focus spot profile of RIAPL with the 8-divided waveplate and (c) RILPL without the waveplate.

The pulse with a few percent of the laser energy was split by a pellicle and is converted to second harmonic ($\lambda \sim 400$ nm, $\tau \sim 50$ fs) by beta-barium borate (β-BaB$_2$O$_4$, BBO) crystal. This second harmonic is used as probe pulse to observe the condition of plasma by shadowgraph imaging from the side. At the upper side of the gas jet, an optical spectrometer is placed to observe spectrum of the side scattering from the laser plasma interactions. The spectral range of the optical spectrometer is from 520 to 1180 nm.

Fig. 2 shows spatially and temporally integrated spectra of side scattering to the normal direction of the laser axis caused by interaction of RIAPL or RILPL with gas jets. One can see significant difference between spectra from RIAPL and RILPL, which is a result of inequality in RIAPL and RILPL propagation in under-dense plasma. While the spectrum generated by an RILPL is a typical for LWFA reflecting the strong red shift owing to
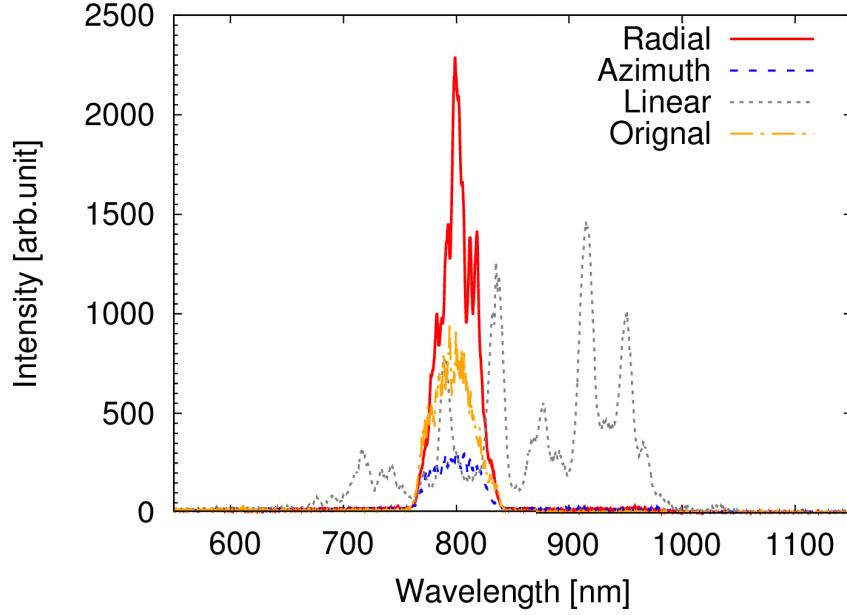
FIG. 2. Spectra of side scattering by using the radially, azimuthally and linearly-polarized pulses and the original spectrum of the laser pulse with pulse energy of 660mJ.

formation of plasma wave in the laser wake[27] and the self-phase modulation by the plasma wave because the pulse width is much longer than the wavelength of plasma wave[28], the spectrum of the RIAPL is slightly broadened around the fundamental wavelength. The bandwidth of the scattering light caused by the RIAPL is almost same as that of the original laser pulse. No signature of wake formation is seen for RIAPL. However, it may be the effect of pulse decomposition: if the RIAPL decomposes during its propagation the scattering light with the red shift may be too weak for detection.

Another sign of RIAPL decomposition during its propagation is exhibited by Fig.3 where (a)-(c) shadowgraph images of the plasmas created by RIAPL and RILPL with a probe pulse (~ 400 nm) and (d)-(e) their profiles after transmission through horizontal polarizer are presented. The probe pulse has the transverse polarization. (a)(d), (b)(e), and (c)(f) show those in the cases of radial polarization, azimuth polarization and linear polarization, respectively. In the shadowgraph images, one can see strong second harmonic (SH) localized near the focus point of RIAPL. This SH has been observed in either case of radial and azimuthal polarizations as shown in Fig. 3(d) and (e).

In contrast to SH emission reported in Ref. [29], in our experiments SH is observed in a quite short distance of about a few tens μm FWHM. In the case of RILPL we did not
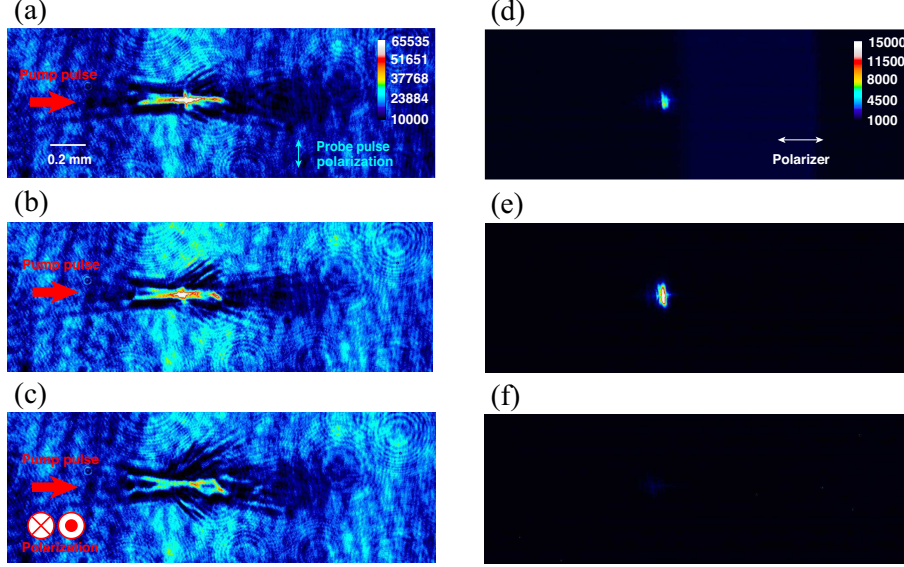
FIG. 3. (a)-(c) Shadowgraph images of the plasmas and (d)-(f) images of the second harmonic source obtained by filtering with polarizer. The probe pulse has the transverse polarization. (a)(d), (b)(e), and (c)(f) show the cases of radial polarization, azimuth polarization and linear polarization, respectively.

observe such strong SH emission in all experiments. Since the probe pulse has the vertical linear polarization it cannot be transmitted through horizontal linear polarizer as in Fig. 3(d)-(f). Therefore, one can see the strong SH emission with different polarization with probe pulse in the cases of the RIAPL.

To analyze the underlying mechanism of the RIAPL pulse propagation and its spectral modification, PIC simulation with FPLaser3D code [30] was performed. The laser pulse and plasma parameters were chosen close to those in the experiments. The axial resolution in the simulation is $\lambda/28$ and the transverse resolution is $\lambda/10$, and 8 particles per cell, where λ is the wavelength of the laser pulse. The plasma length is set to 1 mm, with density gradient of length 120 μm on either edge. The focus position of the pulse is 100 μm inside the simulation box. Fig.4 shows snapshots of the intensity evolution of a radially polarized laser pulse propagating in uniform underdense plasma. Fig.4(a) correspond to 458 fs or 137.4 μm, Fig.4(b) correspond to 817 fs or 245.1 μm, and Fig.4(c) corresponds to 1.86 ps or 558 μm. Simulations reveal that owing to the donut shape of the electric field of the RIAPL pulses, the electron density is compressed along the axial direction. The compressed electron density interacts with the laser pulse and provokes instability. As a
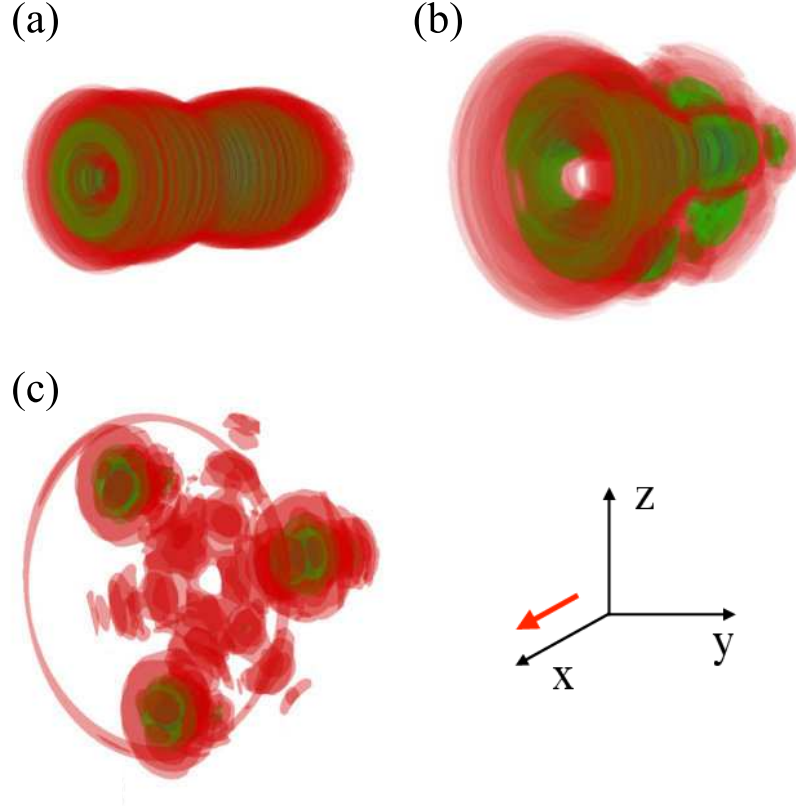
FIG. 4. 3D contour plots of intensity evolution of a radially-polarized pulse propagating in uniform underdense plasma. The snap shots show intensity distribution at (a) 458 fs and (b) 817 fs, and (c) 1.86 ps. The x-y-z triad corresponds to the Cartesian coordinates of the simulation geometry and the arrow indicates the direction of propagation of the pulse.

result of the instability the laser pulse breaks down into filaments. The nature and detailed analysis of this instability can be found in Ref.[20]. Due to compression, the on axis electron density approaches near critical density. Interaction of the laser pulse with such a high density plasma ramp results in harmonic generation[31]. Emission of second harmonic light indirectly implies to the occurrence of the instability. The SH is generated along the density gradient, since the density gradient is perpendicular to the laser pulse direction, the SH emission is observed perpendicular to the pulse propagation direction.

We performed spectral analysis of the laser radiation as a key part of this research using fast fourier transform (FFT). The y-component of the laser electric field transformed from space-domain to k-domain, where k is the wave vector of the laser pulse. Mathematically,
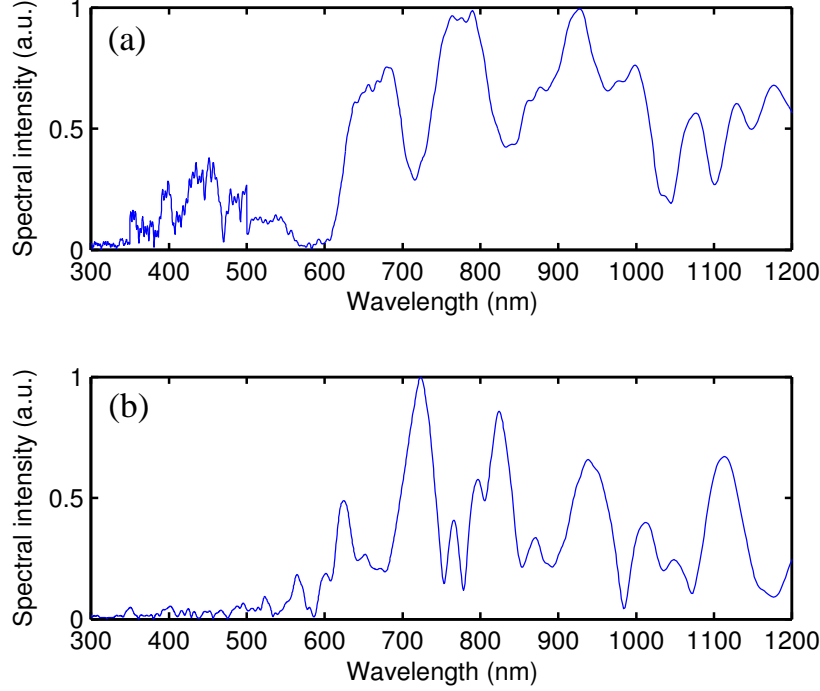
FIG. 5. (a) Spectrum of E_y component of the radially-polarized laser pulse at 1.86 ps, and (2) spectrum of E_y component of the Gaussian laser pulse at 1.86 ps.

this can be written as $f(k) = \sum E_y(x)e^{i2\pi kx}dx$, i.e., the y-component of the laser field is summed up along the y-and z-directions and reduced from 3d to 1d. This total field is than transformed to spectrum using FFT. Fig.5(a) shows the simulated on-axis spectrum of the radially polarized pulse. The spectrum corresponds to Fig.4(c). As expected, there is a clear signal of the second harmonic generation. One can notice that on the one side there is a modulation and progressive red-shift of the laser pulse, which is a sign of wake-field generation, and on the other side, there is a quasi-selective blue-shift of the laser pulse, which is around second harmonic.

To confirm that the generation of the second harmonic radiation is typical for RIAPL pulses, we also performed simulation with Gaussian laser pulse. Fig.5(b) shows the on axis spectrum for the Gaussian pulse at the same time as for the radially polarized laser pulse in Fig.5(a). It displays that there is only red-shift in the simulated spectrum, and no sign of strong second harmonic component. Thus, simulation supports the observation of second harmonic generation from RIAPL pulses in our experimental conditions.

Fig. 6 shows spatial profiles of electron beams generated by the RIAPL (radial and

azimuth polarizations) and the RILPL with pulse energies 660 mJ on target. As shown in Fig.6 (a) and (b), the divergence of the electron beam in the case of the RIAPLs is smaller than the RILPL in Fig.6(c). The electron number on the center of beam produced by the RIAPL is more than the RILPL. Energy spectra of the electron beams with each polarization are also shown in Fig. 6(d). The temperature of the electron beam produced by the RIAPL is lower than the RILPL. It could be caused by slightly lower intensity of the RIAPL than the RILPL. In the acceleration by RIAPL, pre-pulse effect may drastically change the acceleration process: according to Ref.[20] there is no RIAPL decomposition in plasma channels. In the present experiments we worked with a short-focus laser pulse and a short gas jet which length is $\sim$ 1 mm. Therefore in electron spectra we see distributions of self-injected electrons without further acceleration in the case of RIAPL. Since the electron self-injection occurs mostly in the vicinity of focus spot we observe no significant difference in LWFA with RILPL and RIAPL. An increase of gas jet length and the pre-pulse energy may drastically change this result.

In conclusion, we have found experimental proof of strong decomposition of axisymmetrically-polarized laser pulses in under-dense plasma. During the decomposition the strong SH is emitted in quite short distance. In the case of linearly-polarized laser pulses SH emission does not occur. The SH emission confirms the electron compression near the laser axis that results in the pulse instability. Due to pulse decomposition no notable red shift was observed in time- and space-integrated spectra of scattering light. Therefore, no essential laser wakefield acceleration of plasma electrons has been observed. Detected MeV energy electrons are the results of wake wave decomposition only. However, RIAPL can propagate in deep plasma channels without the decomposition[20]. This means that the RIAPL can be used for probing the plasma optical elements[30]. For example exit of RIAPL from a plasma channel will be accompanied by a strong emission of SH which is easy to detect.
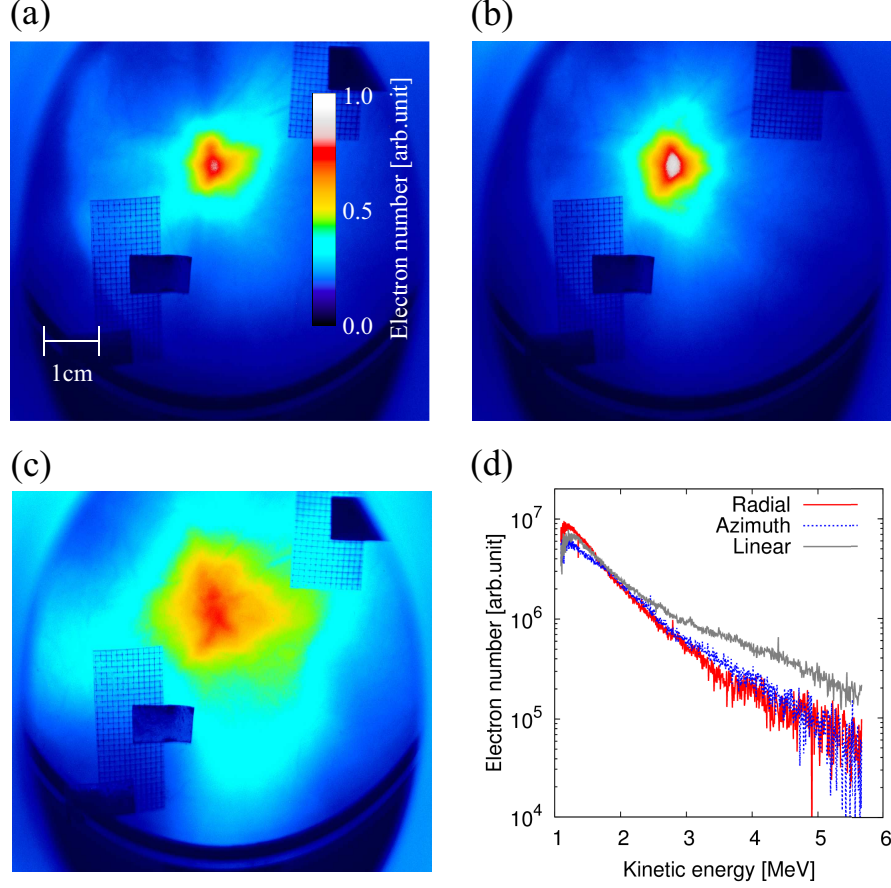
FIG. 6. Spatial profiles of electron beams in the case of (a) radial, (b) azimuthal, and (c) linear polarization with pulse energy of 660mJ, and (d) energy spectra of electron beams for each polarization.

[1] S. P. D. Mangles, C. D. Murphy, Z. Najmudin, A. G. R Thomas, J. L.Collier, A.E. Dangor, P. S. Foster, J. L. Collier, E. J. Divall, J. G.Gallacher, C. J. Hooker, D. A. Jaroszynski, A. J. Langley, W. B. Mori, P. A. Norreys, F. S. Tsung, R. Viskup, B. R. Walton and K. Krushelnick, Nature **431**, 535 (2004).

[2] C. G. R. Geddes, Cs. Toth, J. van Tilborg, E. Esarey, C. B. Schroeder, D. Bruhwiler, C. Nieter, J. Cary, and W. P. Leemans, Nature **431**, 538 (2004).

[3] J. Faure, Y. Glinec, A. Pukhov, S. Kiselev, S. Gordienko, E. Lefebvre, J.-P. Rousseau, F. Burgy, and V. Malka, Nature **431**, 541 (2004).

[4] E. Miura, K. Koyama, S. Kato, N. Saito, M. Adachi, Y. Kawada, T. Nakamura and M. Tanimoto, Appl. Phys. Lett. **86**, 251501 (2005).

[5] W. P. Leemans, B. Nagler, A. J. Gonsalves, C. Toth, K. Nakamura, C. G. R. Geddes, E. Esarey, C. B. Schroeder, and S. M. Hooker, Nat. Phys. **2**, 696 (2006).

[6] S. Karsch, J. Osterhoff, A. Popp, T. P. Rowlands-Rees, Zs. Major, M. Fuchs, B. Marx, R. Horlein, K. Schmid, L. Veisz, S. Becker, U. Schramm, B. Hidding, G. Pretzler, D. Habs, F. Gruner, F. Krausz, and S. M. Hooker, New J. Phys. **9**, 415 (2007).

[7] X. Wang, R. Zgadzaj, N. Fazel, Z. Li, S. A. Yi, Xi Zhang, W. Henderson, Y.-Y. Chang, R. Korzekwa, H.-E. Tsai, C.-H. Pai, H. Quevedo, G. Dyer, E. Gaul, M. Martinez, A. C. Bernstein, T. Borger, M. Spinks, M. Donovan, V. Khudik, G. Shvets, T. Ditmire and M. C. Downer, Nat Comm. **4**, 1988 (2013).

[8] W. P. Leemans, A. J. Gonsalves, H.-S. Mao, K. Nakamura, C. Benedetti, C. B. Schroeder, Cs. Toth, J. Daniels, D. E. Mittelberger, S. S. Bulanov, J.-L. Vay, C. G. R. Geddes, and E. Esarey, Phys. Rev. Lett. **113**, 245002 (2014).

[9] K. Krushelnick, Z. Najmudin, S.P.D. Mangles, A.G.R. Thomas, M.S. Wei, B. Walton, A. Gopal, E.L. Clark, A.E. Dangor, S. Fritzler, C.D. Murphy, P.A. Norreys, W.B. Wei, J. Gallacher, D. Jaroszynski, and R. Viskup, Phys. Plasmas **12**, 056711 (2005).

[10] D. Kaganovich, A. Ting, D. F. Gordon, R. F. Hubbard, T. G. Jones, A. Zigler, and P. Sprangle, Phys. Plasmas **12**, 100702 (2005).

[11] W. D. Kimura, A. van Steenbergen, M. Babzien, I. Ben-Zvi, L.P. Campbell, D.B. Cline, C.E. Dilley, J.C. Gallardo, S.C. Gottschalk, P. He, K.P. Kusche, Y. Liu, R.H. Pantell, I.V. Pogorelsky, D.C. Quimby, J. Skaritka, L.C. Steinhauer, and V. Yakimenko, Phys. Rev. Lett. **86**, 4041 (2001).

[12] T. Tajima, Proc. Jpn. Acad. Ser. B Phys. Biol. Sci. **86**, 147 (2010).

[13] W. L. Kruer, *The physics of laser plasma interaction*, Addison Wesley (1998).

[14] C. S. Liu and V. K. Tripathi, *The interaction of electromagnetic waves with electron beams and plasmas*, World Scientific (1994)

[15] P. Gibbon, *Short pulse laser interaction with matter*, World Scientific (2005).

[16] S. Takeuchi, R. Sugihara and K. Shimoda, J. Phys. Soc. Jpn. **63**, 1186 (1994).

[17] E. Esarey, P. Sprangle and J. Krall, Phys. Rev. E **52**, 5443 (1995).

[18] Q. Kong, S. Miyazaki, S. Kawata, K. Miyauchi, K. Nakajima, S. Masuda, N. Miyanaga and Y. K. Ho, Phys. Plasmas **10**, 4605 (2003).

[19] J. Vieira and J. T. Mendonca, Phys. Rev. Lett. **112**, 215001 (2014).

[20] N. Pathak, A. Zhidkov, N. Nakanii, S. Masuda, T. Hosokai, and R. Kodama, Phys. Plasmas **23**, 033102 (2016); arXiv:1510.07374 (2015).

[21] H. Tomizawa and M. Kobayashi, Proc. FEL2007, **382** (2007).

[22] A. Maekawa, M. Uesaka and H. Tomizawa, Proc. FEL2008, **435** (2008).

[23] T. Hosokai, K. Kinoshita, A. Zhidkov, A. Maekawa, A. Yamazaki, and M. Uesaka, Phys. Rev. Lett. **97**, 075004 (2006).

[24] T. Hosokai, A. Zhidkov, A. Yamazaki, Y. Mizuta, M. Uesaka, and R. Kodama, Appl. Phys. Lett. **96**, 121501 (2010).

[25] N. Nakanii, T. Hosokai, K. Iwasa, S. Masuda, A. Zhidkov, N. Pathak, H. Nakahara, Y. Mizuta, N. Takeguchi and R. Kodama, Phys. Rev. ST-AB **18**, 021303 (2015).

[26] S.V. Bulanov, I. N. Inovenkov, V. I. Kirsanov, N. M. Naumova, and A. S. Sakharov, Phys. Fluids B **4**,1935 (1992).

[27] A. Giulietti et al., Phys. Plasmas **20**, 082307 (2013).

[28] V. Malka, A. Modena, Z. Najmudin, A.E. Dangor, C.E. Clayton, K. A. Marsh, C. Joshi, C. Danson, D. Neely and F.N. Walsh, Phys. Plasmas **4**, 1127 (1997).

[29] Y. Mizuta, T. Hosokai, S. Masuda, A. Zhidkov, K. Makito, N. Nakanii, S. Kajino, A. Nishida, M. Kando, M. Mori, H. Kotaki, Y. Hayashi, S.V. Bulanov and R. Kodama, Phys. Rev. ST-AB **15**, 121301 (2012).

[30] A. G. Zhidkov, T. Fujii, and K. Nemoto, Phys. Rev. E **78**, 036406 (2008).

[31] J. A. Stamper, R. H. Lehmberg, A. Schmitt, M. J. Herbst, F. C. Young, J. H. Gardner, and S. P. Obenschain, Phys. Fluids **28**, 2563 (1985)